AMERICAN SOCIETY FOR MICROBIOLOGY | Journal of Bacteriology®

RESEARCH ARTICLE

The Conserved Translation Factor LepA Is Required for Optimal Synthesis of a Porin Family in *Mycobacterium smegmatis*

Skye R. S. Fishbein,[a] Francesca G. Tomasi,[a] Ian D. Wolf,[a] Charles L. Dulberger,[a] Albert Wang,[a] Hasmik Keshishian,[b] Luke Wallace,[b] Steven A. Carr,[b] Thomas R. Ioerger,[c] E. Hesper Rego,[d] Eric J. Rubin[a]

[a]Department of Immunology and Infectious Disease, Harvard TH Chan School of Public Health, Boston, Massachusetts, USA
[b]Broad Institute of MIT and Harvard, Cambridge, Massachusetts, USA
[c]Department of Computer Science and Engineering, Texas A&M University, College Station, Texas, USA
[d]Department of Microbial Pathogenesis, Yale University School of Medicine, New Haven, Connecticut, USA

ABSTRACT The recalcitrance of mycobacteria to antibiotic therapy is in part due to its ability to build proteins into a multilayer cell wall. Proper synthesis of both cell wall constituents and associated proteins is crucial to maintaining cell integrity, and intimately tied to antibiotic susceptibility. How mycobacteria properly synthesize the membrane-associated proteome, however, remains poorly understood. Recently, we found that loss of *lepA* in *Mycobacterium smegmatis* altered tolerance to rifampin, a drug that targets a nonribosomal cellular process. LepA is a ribosome-associated GTPase found in bacteria, mitochondria, and chloroplasts, yet its physiological contribution to cellular processes is not clear. To uncover the determinants of LepA-mediated drug tolerance, we characterized the whole-cell proteomes and transcriptomes of a *lepA* deletion mutant relative to strains with *lepA*. We find that LepA is important for the steady-state abundance of a number of membrane-associated proteins, including an outer membrane porin, MspA, which is integral to nutrient uptake and drug susceptibility. Loss of LepA leads to a decreased amount of porin in the membrane, which leads to the drug tolerance phenotype of the *lepA* mutant. In mycobacteria, the translation factor LepA modulates mycobacterial membrane homeostasis, which in turn affects antibiotic tolerance.

IMPORTANCE The mycobacterial cell wall is a promising target for new antibiotics due to the abundance of important membrane-associated proteins. Defining mechanisms of synthesis of the membrane proteome will be critical to uncovering and validating drug targets. We found that LepA, a universally conserved translation factor, controls the synthesis of a number of major membrane proteins in *M. smegmatis*. LepA primarily controls synthesis of the major porin MspA. Loss of LepA results in decreased permeability through the loss of this porin, including permeability to antibiotics like rifampin and vancomycin. In mycobacteria, regulation from the ribosome is critical for the maintenance of membrane homeostasis and, importantly, antibiotic susceptibility.

KEYWORDS LepA, ribosome, mycobacteria, porin, drug susceptibility

Mycobacterium tuberculosis, the causative agent of tuberculosis (TB), is refractory to treatment with a single antibiotic and, despite combination therapy, widespread multidrug resistance is a growing concern (1, 2). New therapeutic approaches are required to subvert both tolerance and outright drug resistance in mycobacteria. In addition to establishing cell integrity and facilitating nutrient import, the mycobacterial cell wall and its outer membrane serve as critical determinants of mycobacterial drug tolerance and susceptibility (3–5). Given the relationship between the cell wall and intrinsic antibiotic susceptibility, a more complete understanding of the genetic networks that affect its construction will facilitate the development of new therapeutics.

Citation Fishbein SRS, Tomasi FG, Wolf ID, Dulberger CL, Wang A, Keshishian H, Wallace L, Carr SA, Ioerger TR, Rego EH, Rubin EJ. 2021. The conserved translation factor LepA is required for optimal synthesis of a porin family in *Mycobacterium smegmatis*. J Bacteriol 203:e00604-20. https://doi.org/10.1128/JB.00604-20.

Editor Tina M. Henkin, Ohio State University

Address correspondence to Eric J. Rubin, erubin@hsph.harvard.edu.

Received 10 November 2020
Accepted 15 December 2020
Accepted manuscript posted online 23 December 2020
Published 22 February 2021

The synthesis and remodeling of the mycobacterial cell wall lipid/peptidoglycan components are highly regulated (6), yet little is understood about how the membrane-associated proteome is properly synthesized. In bacteria, recent advances in techniques such as quantitative proteomics, ribosome profiling, and cryo-electron microscopy (cryo-EM) have revealed that an additional layer of regulation during protein synthesis serves to maintain cellular homeostasis (7, 8) and enable appropriate synthesis of membrane proteins (9). With this increased resolution, it is clear that ribosome function can be altered by proteins and RNA factors that associate to them in a message- and environment-specific manner (10, 11). These associating factors help to control translation rate, protein folding, and localization, ultimately contributing to a cell with a spatially and temporally regulated proteome (12–14).

In mycobacteria, it is plausible that regulation at the ribosome may contribute to pathogenicity and drug susceptibility (15). Studies of ribosome-associated proteins such as HflX, Mpy, and LepA have linked these factors to drug tolerance in both *M. tuberculosis* and *M. smegmatis* (16–18). While some of these enzymes have clear roles in ribosome stability and hibernation, less is known about how LepA associates with the mycobacterial ribosome and affects drug tolerance (19). Specifically, the link between LepA and antibiotic tolerance in mycobacteria was uncovered in a screen for genetic determinants of single-cell heterogeneity and drug susceptibility. Mutations in several genes, including *lepA*, altered the rate of antibiotic-mediated killing (18).

LepA is a ribosome-dependent GTPase found in almost all organisms, from bacteria to human mitochondria (19, 20). It uses four classical elongation factor protein domains to contact the ribosome and hydrolyze GTP, occupying the same position on the 70S ribosome as elongation factor G (EF-G) (21). It is nonessential in most bacteria, but it has been speculated that LepA may confer a fitness benefit in certain growth conditions, such as altered cation concentrations or low pH (22–27). Despite its conservation, the physiological role of LepA remains unclear, as underlined by two different proposed roles for this GTPase. In *Escherichia coli*, loss of LepA results in decreased polysome formation, suggesting a role in initiation and ribosome assembly (27–29). Alternatively, structural studies on multiple bacterial LepA homologs indicate that its C-terminal domain makes contact with the A/P-site tRNA of the 70S ribosome and may alter the conformation of the ribosome-tRNA complex (30, 31), perhaps participating in translational quality control (29, 32, 33).

Here, we investigate the mechanistic basis of altered drug susceptibility of a mycobacterial *lepA* deletion mutant. We find that LepA augments protein levels for certain members of the mycobacterial porin (Msp) family during translation, as well as a number of other membrane-associated proteins. LepA deficiency results in decreased synthesis of MspA, the major porin in *M. smegmatis*, and a reduction in cell permeability as measured by dye accumulation and killing by certain antibiotics. Thus, we find that LepA acts as a translational aid in mycobacteria, providing evidence for its role in maintenance of prominent members of the mycobacterial membrane proteome, and demonstrating ribosome-based control of membrane homeostasis.

RESULTS

Loss of LepA results in mycobacterial drug tolerance through its activity at the ribosome. In a previous screen, we found that strains carrying transposon insertions in *lepA* were predicted to be associated with decreased accumulation of a fluorescent dye, calcein acetoxymethyl ester (AM), and decreased killing by rifampin, a first-line tuberculosis drug (18, 34). To validate that loss of LepA was responsible for the observed phenotype, we used the *lepA* deletion strain (Δ*lepA*) (18) to generate a complemented strain in which we reintroduced *lepA* in single copy at a phage integration site (Δ*lepA* L5::*lepA*). We found the Δ*lepA* strain exhibited an approximately 2-fold decrease in calcein signal (Fig. 1A) relative to the wild-type (WT) and complemented strains. Loss of LepA also resulted in increased tolerance to rifampin and vancomycin (see Fig. 1B and C) (18), but had no effect on tolerance to isoniazid or linezolid (see Fig. S1A and B in the

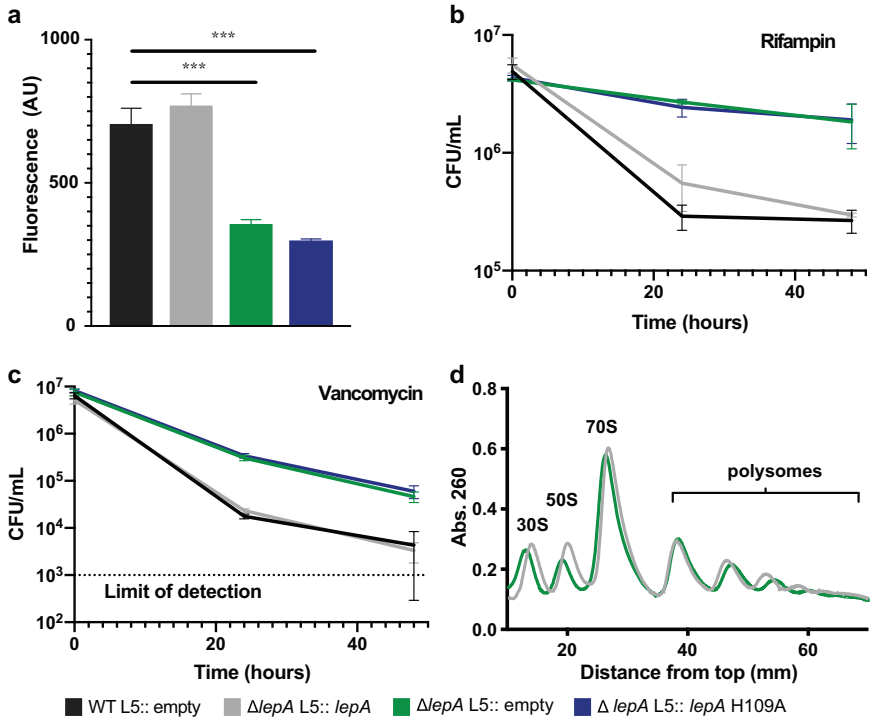

FIG 1 Loss of ribosome factor LepA causes altered drug tolerance in mycobacteria. (a) Calcein staining across *M. smegmatis* strains with different *lepA* alleles. Values indicate mean calcein fluorescence across three replicates with error bars indicating standard deviation. ***, $P < 0.001$, calculated using a two-sided Student *t* test. (b and c) *M. smegmatis lepA* strains were treated with 10× MICs of rifampin and vancomycin, and cell survival was measured by CFU per milliliter. All values are mean values with error bars indicating standard deviations across three biological replicates. (d) Analysis of ribosome populations by sucrose density centrifugation and fractionation. Distance 0 corresponds to the lightest sucrose fraction. Data in panels a to d are representative of multiple experiments.

supplemental material) or on susceptibility to a variety of translation inhibitors (Table S1).

To define the link between a ribosomal factor and the phenotypes we observed, we first examined LepA's influence on mycobacterial ribosomes and ribosome activity *in vitro*, given its well-studied role as a ribosome-associated GTPase (27, 31, 32). To test whether the GTPase activity of LepA was critical to the phenotypes observed in Δ*lepA* cells, we assayed calcein staining and drug killing with a Δ*lepA* strain complemented with a putative GTPase-null mutant of LepA (Δ*lepA* L5::*lepA* H109A). Mutation of this conserved catalytic histidine was previously shown to abolish LepA GTPase activity in *E. coli* (28). We found that both calcein levels and drug tolerance in the Δ*lepA* L5::*lepA* H109A strain were equivalent to those in the Δ*lepA* strain (Fig. 1A to C), indicating that, in mycobacteria, the GTPase activity of LepA is necessary for both calcein staining and antibiotic tolerance in WT.

We reasoned that LepA could be interacting with the ribosome during ribosome biogenesis, translation initiation, or elongation (23, 24, 28). To determine if mycobacterial LepA altered ribosome biogenesis or stability, we profiled ribosome populations in Δ*lepA* and the complemented strain via sucrose density centrifugation. Unlike in *E. coli*, loss of LepA in *M. smegmatis* did not alter levels of ribosome subunits, assembled 70S, or polysome formation, markers of active translation (Fig. 1D). To directly test mycobacterial LepA activity at the ribosome *in vitro*, we purified *M. smegmatis* LepA and *M. smegmatis* LepA H109A. As previously observed with *E. coli* LepA (19, 28), addition of mycobacterial LepA to an *in vitro* cell-free translation reaction mixture containing Venus mRNA increased Venus signal (Fig. S1C) relative

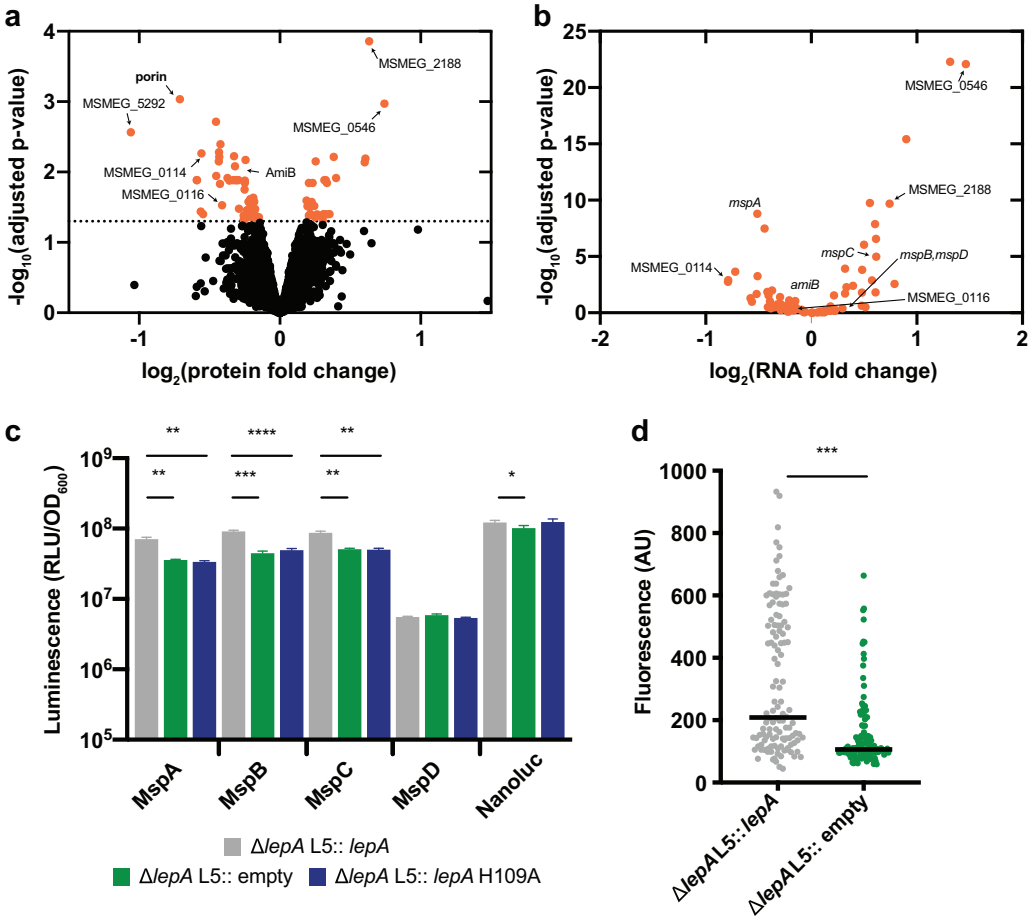

FIG 2 Whole-cell profiling finds mycobacterial porins altered by loss of LepA. (a) Proteins altered by loss of LepA. Log fold changes of protein represent mean reporter ion intensities in Δ*lepA* normalized by mean reporter ion intensities from the strains containing *lepA* (Δ*lepA* L5::*lepA* and wild type [WT] L5:: empty). Orange dots indicate protein candidates that were significantly altered by loss of LepA. "Porin" indicates the collection of peptides that map to 4 proteins: MspA, MspB, MspC, and MspD. *P* values for proteomic ratios were calculated using Student's two-sided *t* test and adjusted for multiple testing using the Benjamini-Hochberg correction with an α of 0.05. (b) Corresponding transcriptional changes in the subset of proteins significantly altered by LepA. Log fold changes and adjusted *P* values for RNA levels were generated using DEseq2.1.8 to analyze the same comparison between strains as in panel a. (c) Luminescence of porin reporters in *M. smegmatis* strains. Mean luminescence is depicted with error bars representing standard deviation of three biological replicates. ***, $P < 0.001$; **, $P < 0.01$; *, $P < 0.05$, calculated using a one-way ANOVA, where each group was compared to the complemented strain, with a Bonferroni correction for multiple testing. (d) Quantification of average fluorescence across a single cell ($n = 100$) from strains expressing MspA-mRFP. ***, $P < 0.001$, calculated using a Mann-Whitney test. Data in panels c and d are representative of multiple experiments.

to the catalytic mutant and control reactions. Our *in vitro* experiments support a role for LepA in active translation rather than in ribosome biogenesis.

Whole-cell profiling of *lepA* mutant reveals dysregulation of outer membrane mycobacterial porins. Based on the altered drug tolerance of the *lepA* mutant, we hypothesized that LepA might affect the translation of proteins that mediate drug susceptibility. To find candidate proteins whose translation was affected by the loss of LepA, we measured simultaneous steady-state levels of proteins and transcripts from wild type, the deletion mutant, and the complemented strain. Given multiple phenotypes demonstrating that the wild type and the complemented strain are physiologically comparable relative to Δ*lepA*, we compared protein and RNA levels between strains with LepA (Δ*lepA* L5::*lepA* and WT) and without LepA (Δ*lepA*).

To quantify the relative abundance of proteins, we used tandem-mass-tag (TMT) labeling of peptides, after tryptic digestion of cell lysates, coupled with liquid chromatography-tandem mass spectrometry (LC-MS/MS). We identified a total of 4,646 proteins with 4,549 of them quantified by 2 or more peptides (Data Set S1). Among these 4,549 proteins, 78 were significantly altered by the loss of LepA (Fig. 2A). Interestingly, a number of membrane processes were enriched in the subset of proteins altered by LepA (Fig. S2A) (35). One of the most significant changes in the Δ*lepA* strain was the

decreased abundance of peptides corresponding to a highly similar set of four porins: MspA, -B, -C, and -D (Fig. S2B). Mycobacterial porins are octameric channels built into the mycomembrane and are responsible for the uptake of nutrients critical for mycobacterial growth (36–39). The four porins in *M. smegmatis*, encoded by *mspA* to *mspD*, are paralogs distributed across the genome. Each porin transcript encodes a Sec signal peptide that enables cotranslational targeting of these proteins into the mycobacterial membrane (40, 41).

We used RNA sequencing (RNA-seq) to estimate the transcriptional contribution to the set of regulated proteins from our proteomics (Data Set S2). Despite finding a number of mRNAs encoding membrane proteins to be increased in the Δ*lepA* strain, transcript levels across the four porin transcripts were altered in both directions, which was not consistent with our observation of the bulk decrease in protein levels of the porin family (Fig. 2B). To precisely measure the levels of each porin transcript, we used quantitative RT-PCR (RT-qPCR) and, indeed, found that none were significantly altered by loss of *lepA* (Fig. S2C). Together, these data show that loss of *lepA* leads to a disproportionate decrease in porin-derived peptides compared to their encoding transcripts.

LepA increases the abundance of a subset of mycobacterial membrane proteins. As our whole-cell proteomics data identified peptides that mapped to all four porins, we sought to identify the porin whose translation was most affected by LepA. We fused each protein to a C-terminal luciferase reporter and expressed the fusions in single copy in a merodiploid, a strain that continues to produce the wild-type copies of each protein. Using luminescence levels as a proxy for protein abundance, we examined levels of each porin in the presence of functional LepA, the GTPase mutant, or the knockout strain. The presence of functional LepA, but not the GTPase mutant, increased luminescence 2- to 3-fold for fusions with coding sequences of MspA, MspB, and MspC but not for MspD or luciferase alone (Fig. 2C). Additionally, we used the luciferase fusion approach to test other candidates that were significantly altered at the protein level and found that a cell wall amidase (AmiB) and an ABC transporter-associated protein (MSMEG_0114) were significantly increased by the presence of *lepA*, as indicated by reporter fusion experiments (Fig. S2D).

As the Msp porins are known to mediate drug susceptibility, likely through intracellular drug accumulation (42, 43), we hypothesized that LepA's influence on porin abundance could explain the *lepA* phenotypes. To verify the function of our porin reporter fusions, we used fluorescence microscopy to examine the location of an MspA-monomeric red fluorescent protein (mRFP) fusion relative to proteins with known or predicted localization patterns. For this comparison, we used fusions of the fluorescent protein Dendra2 to GroEL, a cytoplasmic protein, and MmpL3, a membrane protein (Fig. S3A). We observed that MspA-mRFP had localization strongly suggestive of membrane association, characterized by a halo of fluorescence around the cell body and an absence of signal along the medial axis. In addition, we found that an MspA-mRFP fusion is less abundant at the membrane in the absence of LepA (Fig. 2D), an observation that supports the findings from the luciferase fusion studies. These data support our hypothesis that LepA acts as a ribosomal GTPase to improve synthesis of a number of mycobacterial porins into the mycobacterial membrane.

LepA affects membrane permeability through control of major porin MspA. What is the physiological cost of decreased synthesis of each porin in the absence of LepA? To understand this, we employed an inducible CRISPRi strategy to transcriptionally deplete each porin individually (Fig. S3B) (44). To assess permeability, we compared calcein fluorescence of each porin knockdown in the presence or absence of LepA. Of the four porins tested, only depletion of MspA eliminated the LepA-dependent increase in calcein signal (Fig. 3A). Correspondingly, expressing higher levels of MspA, but not MspD, in the presence of *lepA* increased calcein staining (Fig. S3C). In contrast, MspD did not increase the permeability in either genetic background. These data suggest that LepA-mediated regulation of MspA abundance during translation is primarily responsible for the observed *lepA* deletion phenotypes.

We reasoned that if *mspA* and *lepA* were functioning in the same pathway, we should

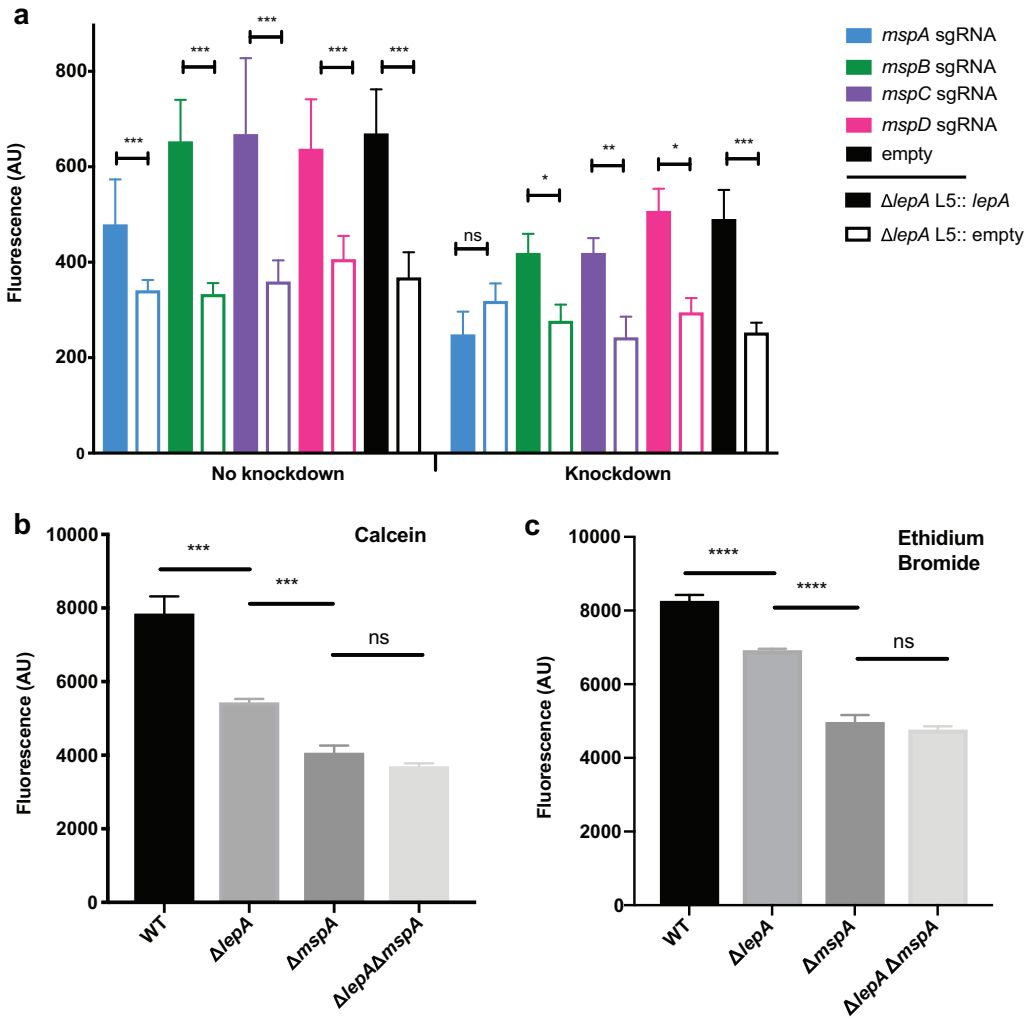

FIG 3 Loss of LepA causes membrane defects primarily through control of MspA. (a) Calcein staining of *lepA*-porin genotypes. Knockdown of each porin was assessed in *lepA* strains. Mean fluorescence is depicted with error bars indicating standard deviations across three biological replicates. Sets of colored bars denote porin-specific knockdown strains. "Empty" refers to strains containing the control vector with the aTc-inducible CRISPRi system and no target-specific small guide RNA (sgRNA). ***, $P < 0.001$; **, $P < 0.01$; *, $P < 0.05$; ns, not significant; calculated using a two-sided Student *t* test. (b) Calcein fluorescence across *M. smegmatis* strains, with error bars indicating standard deviations across three biological replicates. (c) EtBr fluorescence across *M. smegmatis* strains, with error bars indicating standard deviations across three biological replicates. ****, $P < 0.0001$; ***, $P < 0.001$; ns, not significant, calculated using a one-way ANOVA. Data in panels a to c are representative of multiple experiments.

be able to detect this by epistasis experiments using a number of reporters of permeability (45). Accordingly, we deleted *mspA* in the original *lepA* deletion strain and measured fluorescence of both calcein and ethidium bromide (EtBr) in our mutants. We found that the loss of both genes does not lead to a more severe reduction in calcein or EtBr accumulation than in the single *mspA* mutant (Fig. 3B and C). Thus, *lepA* is epistatic to *mspA* in *M. smegmatis*, suggesting that they function in the same pathway. Together, these data indicate that while LepA is sufficient to affect the translation of multiple porins, it mainly controls the synthesis of MspA, which in turn mediates permeability to multiple compounds, including antibiotics.

DISCUSSION

LepA is highly conserved across the kingdoms of life, yet its cellular role remains unclear. While *lepA* mutants are viable, they have a very specific permeability defect.

Considering our data and that of others suggesting that porins are important for drug accessibility (18, 46), it is unsurprising that both *lepA* and *mspA* mutants are less susceptible to rifampin and vancomycin. This change in uptake could be due to either indirect changes to outer membrane permeability resulting from loss of porin, or to direct decreases in drug transport through the porin itself. In fact, changes in MspA function alter the transport of a large number of nutrients across the cell wall (41, 47–49). Our data also suggest that LepA aids the translation of other membrane-associated proteins, namely, AmiB, a cell wall amidase, and a member of a putative taurine transport operon, MSMEG_0114 (see Fig. S2 in the supplemental material). Furthermore, we found a number of membrane proteins whose levels increased in the absence of LepA (Data Set S1). We hypothesize that these changes are a compensatory response to the loss of the major porin family in *M. smegmatis*, either through transcriptional changes or some unknown regulatory mechanism. Decreased nutrient uptake due to loss of porins may trigger the upregulation of a number of alternative processes to compensate for nutrient import. Alternatively, if LepA works in concert with the Sec translocon, loss of LepA could skew the balance of ribosome activity toward some other secretion machinery.

A number of observations from genome-wide transposon screens in mycobacteria suggest that LepA's function centers around membrane processes. In *M. tuberculosis*, *lepA* becomes essential for growth in the absence of *ponA1*, a prominent cell wall biosynthetic enzyme in *M. tuberculosis* (50). Loss of cell wall enzymes like PonA1 may result in collateral perturbation to the membrane proteome, causing LepA to become indispensable. Further, while *lepA* is nonessential for *in vitro* growth of *M. tuberculosis*, *lepA* transposon mutants grow poorly during murine infection (51). *M. tuberculosis* requires a number of different membrane complexes during infection (52, 53), and we speculate that LepA-dependent synthesis of membrane processes is required for survival *in vivo*. Finally, there is evidence both in mycobacteria and *E. coli* that the synthesis of outer membrane porins and cell wall amidases is tightly regulated (34, 54). LepA function in mycobacteria appears to be critical for maintenance of the mycomembrane, the complex network of lipids and proteins that coordinate cellular processes ranging from cell division to nutrient transport (Fig. 4) (5).

How does LepA control the abundance of MspA? Unlike in *E. coli*, LepA does not alter the distribution of ribosomal subunits and assembled ribosomes in mycobacteria (28, 29). *In vitro*, LepA increased translation, indicating that it functions with assembled ribosomes. While we cannot rule out specific ribosomal protein defects from altered biogenesis (29), LepA's role in porin synthesis and our observations *in vitro* lead us to conclude that, in a mycobacterial cell, LepA acts during translational elongation. LepA has been shown to have 70S-dependent GTPase activity, and its binding affinity to the ribosome is increased by its C-terminal domain (55). The GTPase mutant's lack of activity *in vitro* and inability to complement the Δ*lepA* phenotype or increase porin abundance supports the model that LepA acts at the 70S ribosome to augment porin levels (Fig. 4D). As structural studies in *E. coli* suggest there is no direct interaction between LepA and mRNA, some other mechanism, such as sensing ribosomal conformation or interaction with secretion machinery, likely underlies LepA function. Alternatively, mycobacterial LepA may have a distinct interaction with the mycobacterial ribosome relative to the well-studied LepA homologs.

We propose two possible roles for LepA as a translational elongation factor in *M. smegmatis*: (i) in quality control for abundant mRNAs and (ii) in membrane protein synthesis. In *M. smegmatis*, *mspA* is one of the most abundant transcripts in the cell (Table S2) (56). Often, highly transcribed mRNAs are also highly translated in bacteria (57). While we do not find evidence of a relationship between RNA levels and LepA influence, we think it is appropriate to discuss the implications of translational control of an abundant message. As LepA competes with EF-G for ribosome binding (from work in *E. coli*), it is possible that, at least for abundant messages, LepA acts as a quality control elongation factor that facilitates the continued and efficient synthesis of messages that demand a large pool of ribosomes. Loss of this factor could impact the translation rate

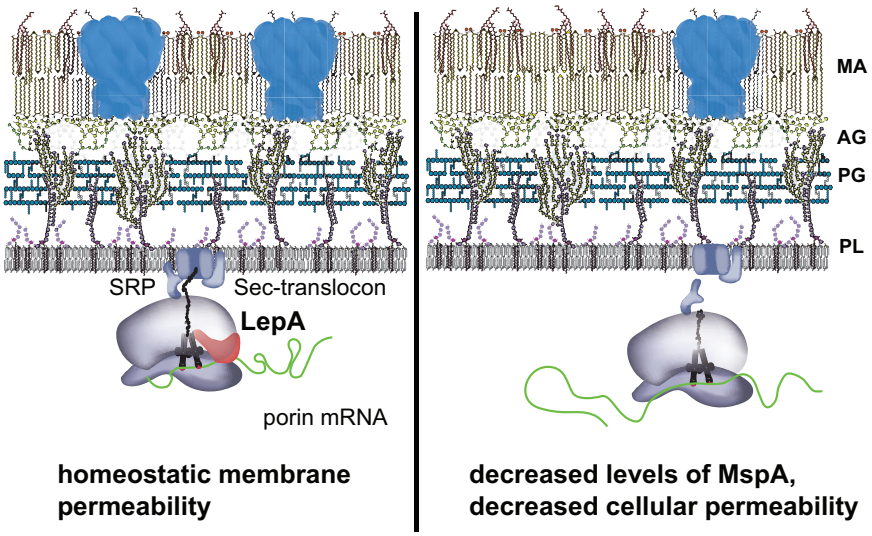

FIG 4 Model of LepA modulation of porin translation. LepA aids translation of outer membrane porins, most notably MspA, and determines permeability and drug susceptibility in *M. smegmatis*. MA, mycolic acids; AG, arabinogalactan; PG, peptidoglycan; PL, phospholipids; SRP, signal recognition particle.

and, thus, cotranslational folding for highly abundant messages. In the case of porins, this delay might exacerbate a nascent polypeptide's ability to be recognized by the secretory system or other posttranslational factors. While LepA may have roles beyond the translation of membrane proteins, studies of translation in other organism suggest a necessity for strict translational control of membrane proteins (58–61). LepA may also therefore be involved directly at the Sec translocon. Given the complexity of the mycobacterial cell wall, we hypothesize that LepA is one of a number of regulatory mechanisms that interact to properly synthesize cell wall-associated proteins. Our findings also align with observations from eukaryotic organelles, whereby LepA appears to influence the levels of critical membrane-bound respiration and photosystem complexes (22, 23, 27, 62).

Pathogenic mycobacteria are intrinsically resistant to antibiotics and require combination therapies. Additionally, acquired drug resistance is a growing concern that demands urgent efforts to develop new treatments. For mycobacteria, defining the mechanisms by which the cell builds its membrane proteome is critical to identifying pathways that encode innate antibiotic resistance. We expect that mycobacteria utilize other forms of posttranscriptional control to build their membrane proteome. Thus, better understanding the interplay of cellular regulatory networks will inform antibiotic discovery efforts.

MATERIALS AND METHODS

Bacterial strains and growth conditions. *M. smegmatis* strains were inoculated from frozen stocks into Middlebrook 7H9 medium supplemented with 0.2% glycerol, 0.05% Tween 80, and ADC (5 g/liter bovine serum albumin, 2 g/liter dextrose, 3 μg/ml catalase) and grown at 37°C. Appropriate antibiotics or inducing agents were used at the following concentrations in *M. smegmatis*: nourseothricin (Nat; 20 μg/ml), zeocin (Zeo; 20 μg/ml), kanamycin (Kan; 25 μg/ml), hygromycin B (Hyg; 50 μg/ml), and anhydrous tetracycline (aTc; 100 ng/ml). Transformations, performed for the construction of *M. smegmatis* strains, were plated onto LB agar plates supplemented with the appropriate antibiotic. Unless otherwise specified for an experiment, strains were grown to log phase (optical density at 600 nm [OD_{600}] of 0.3 to 0.8) without antibiotics. For cloning purposes, *E. coli* strains were grown in LB broth or on LB agar with antibiotics as follows: Nat (40 μg/ml), Zeo (50 μg/ml), Kan (25 μg/ml), and Hyg (100 μg/ml).

Bacterial strain construction. All bacterial strains constructed in this study can be found in Table S2 in the supplemental material. Description of the plasmids, primers, and recombinant DNA used to construct the strains can be found in Tables S3, S4, and S5, respectively. Generally, all plasmids were constructed by restriction digestion of the parental vector (with the desired antibiotic resistance gene and phage integration gene for *M. smegmatis* propagation) and all inserts were prepared by amplifying gene fragments with 18- to 25-bp Gibson assembly overhangs. Vector and insert combinations were ligated together by Gibson isothermal assembly (63). Plasmids were isolated from *E. coli* and insert orientation was sequenced via Sanger sequencing. Sequencing reactions were carried out with an ABI3730xl DNA analyzer at the DNA Resource Core of Dana-Farber/Harvard Cancer Center.

Deletion mutants. The *lepA* mutant, the Δ*lepA*::*zeo* strain (HR334), and the *mspA* mutant, the

Δ*mspA*::*zeo* strain (HR329), were previously constructed (18). The Δ*lepA*::*zeo* Δ*mspA*::*hyg* strain (SF789) was constructed with HR334 as the parental strain, using double-stranded recombineering. For recombination, a linear double-stranded DNA (dsDNA) fragment was generated by amplifying the following fragments: the 500-bp upstream region of *mspA*, the 500-bp downstream region of *mspA*, and a *lox-hyg-lox* fragment. The three fragments were ligated together using Gibson assembly. The deletion cassette was transformed into a Δ*lepA* recombineering strain as previously described (64, 65) and plated on Hyg to select for double mutants.

***lepA* and *mspA* alleles.** Plasmid pSF121, used for *lepA* complementation, was generated using a parental vector (pCT94) that integrates into the L5 phage site and is marked with a Kan resistance (*kan*) gene. The vector was digested with XbaI and HindIII (New England BioLabs, Ipswitch, MA). *lepA* and its 5′ untranslated region (UTR; 300 bp upstream) were amplified via PCR. The vector and insert were gel extracted and ligated using Gibson assembly. The complemented strain (SF178 Δ*lepA*::*zeo* L5::*lepA-kan*) and the marked mutant Δ*lepA* strain (SF181 Δ*lepA*::*zeo* L5::empty-*kan*) were derivatives of HR334. Plasmid pSF417, used for *lepA* complementation in the CRISPRi experiments, was generated using a parental vector (pCT204) that integrates at the Tweety (Tw) phage integration site and is marked with a Hyg resistance (*hyg*) gene. The *lepA* insert was amplified from the *M. smegmatis* genome as above, and the parental vector was linearized by digesting with SspI and NdeI. The resulting vector was assembled as above.

For microscopy, *mspA* was fused to monomeric red fluorescent protein (mRFP), with no linker, and constitutively expressed from P_{rpsA}, in a Tw-integrating vector with a nourseothricin resistance (*nat*) gene. The *mspA*-mRFP vector was built using Gibson assembly and transformed into Δ*lepA* and the complemented strain for localization of MspA-mRFP.

Candidate-luciferase fusions. All luciferase reporters were generated from the parental vector CT250, a Tw-integrating vector. The vector was linearized using NdeI and HindIII, to preserve the upstream promoter (P_{rpsA}). For each reporter, the candidate gene was amplified from the *M. smegmatis* genome and the luciferase gene was amplified from a plasmid (pJR976) (44). Using Gibson overhangs that contained glycine-serine-glycine (GSG) linkers, each reporter vector was constructed using Gibson assembly. Each reporter vector was transformed into Δ*lepA* and the complemented strain.

Porin knockdown constructs. Knockdown of each porin was accomplished using mycobacterial CRISPRi, with knockdown systems constructed as previously described (44). Porin knockdown vectors were created by annealing oligonucleotides for each porin and ligating these fragments into a linearized vector (pJR965, digested by BsmBI), containing the mycobacterial CRISPRi system. Knockdown vectors were cotransformed into HR334 with pSF417 or pSF418.

Calcein acetoxymethyl ester (AM) staining. Strains were grown to log phase and stained with 0.5 μg/ml of calcein AM (Invitrogen, Carlsbad, CA) for 1 h. Strains were analyzed by flow cytometry on a MACSQuant (VYB excitation: 488 nm; emission filter: 525/50) in the same manner as previously described (18). Median fluorescence was used from each replicate to compute an overall mean fluorescence intensity.

Kill curves. Strains were grown to mid-log phase, diluted to an OD_{600} of 0.05 and treated with 10× MICs of the following drugs: rifampin (20 μg/ml), isoniazid (40 μg/ml), vancomycin (4 μg/ml), and linezolid (500 ng/ml). Survival was assessed over time as described previously (18).

Drug susceptibility assays. Drug susceptibility was determined using a MIC assay, as described previously (66). In 96-well plates, strains were diluted to 0.005 and tested in biological triplicate in serial dilutions of tetracycline (Sigma-Aldrich, St. Louis, MO), clarithromycin (Sigma-Aldrich, St. Louis, MO), chloramphenicol (Sigma-Aldrich, St. Louis, MO), amikacin (Sigma-Aldrich, St. Louis, MO), and erythromycin (Santa Cruz Biotechnology, Santa Cruz, CA). The highest concentrations of each drug tested were 4 μg/ml for tetracycline, 4 μg/ml for clarithromycin, 320 μg/ml for chloramphenicol, 3.2 μg/ml for amikacin, and 16 μg/ml for erythromycin. Plates were agitated at 37°C for 21 h. To determine MICs for each condition, 0.0002% resazurin was added to each well and plates were agitated at 37°C for 3 h. The first well with no growth (blue) in each concentration gradient was considered the MIC. A biological replicate, in this case, is considered a single row in a 96-well plate of drug and bacterial incubation, using bacteria from the same culture.

Purification of mycobacterial LepA. *M. smegmatis* LepA and LepA H109A were each cloned with an N-terminal 6× His tag using Gibson assembly and expressed from pET28a in BL21 *E. coli*, as previously described for *E. coli* LepA (28). Briefly, 200 ml of log-phase culture was induced with 1 mM isopropyl-β-D-1-thiogalactopyranoside (IPTG) for 4 h at room temperature. Cells were harvested at 5,000 × *g* for 10 min, and pellets were frozen at −80°C overnight. The pellet was lysed at room temperature (RT) for 30 min in BugBuster 10× protein extraction reagent (Millipore Sigma, St. Louis, MO). Cell lysates were clarified by centrifugation at 15,000 × *g* for 30 min at 4°C. Lysate was brought up to 30 mM imidazole, pH 7.6, and His-tagged LepA was extracted via an Ni-nitrilotriacetic acid (Ni-NTA) column (New England BioLabs, Ipswitch, MA) purification. Beads were collected in plastic columns with a 10-ml bed volume and washed with 4 × 10 ml wash buffer (50 mM Tris-HCl [pH 7.6], 300 mM KCl, 5% glycerol, 6 mM β-mercaptoethanol [BME], 30 mM imidazole). One-milliliter elution fractions were collected using elution buffer (50 mM Tris-HCl [pH 7.6], 40 mM KCl, 5% glycerol, 6 mM BME, 200 mM imidazole) and analyzed via SDS-PAGE. The cleanest elution fractions were pooled and dialyzed into 6 liters (3 × 2 liters) of storage buffer (50 mM Tris-HCl [pH 7.6], 50 mM KCl, 5% glycerol, 6 mM BME) using dialysis cassettes with a 10-kDa molecular weight cutoff (MWCO). Aliquots (10 μl) were flash-frozen with liquid nitrogen and stored at –80°C. LepA protein concentration was calculated using the Qubit protein assay kit (Thermo Fisher, Berkeley, MO).

***In vitro* translation.** To assess the effect of LepA on translation, *in vitro* translation reactions were prepared with purified mRNA. Plasmid pSF741 was used in a HiScribe T7 *in vitro* transcription kit (New England BioLabs, Ipswich, MA) to generate Venus mRNA. A master mix of purified Venus mRNA (500 ng per reaction) and PURExpress (New England BioLabs, Ipswich, MA) components was prepared in duplicate reactions with purified *M. smegmatis* LepA or LepA H109A (300 ng per reaction). When no LepA was added to the reaction,

an equal volume of storage buffer was added in place of protein. Reactions were carried out in 20 μl in a 384-well plate for 4 h at 37°C, and fluorescence (measured at an excitation of 505 nm and an emission of 540 nm) was collected on a SpectraMax M2 microplate reader.

Ribosome analysis. Preparation of mycobacterial ribosomes was performed as previously described for *E. coli* (67), yet optimized for *M. smegmatis*. A culture of 500 ml of cells was grown to mid-log phase, filtered over 0.22-μm, 90-mm membranes (Millipore Sigma, St. Louis, MO) on a fritted glass microfiltration apparatus (Kimball-Chase, Rockwood, TN), and scraped into liquid nitrogen. A 500-μl aliquot of lysis buffer (20 mM Tris [pH 8], 10 mM $MgCl_2$, 100 mM NH_4Cl, 5 mM $CaCl_2$, 0.4% Triton X-100, 0.1% NP-40, 34 mg/ml chloramphenicol, 100 U/ml RNase-free DNase I) was added to the cell scrapes. Frozen cells and lysis buffer were ground in a Retsch 400 mixer mill using 10-ml grinding jars and 12-mm grinding balls at 15 Hz for 5 $\times$ 3 min. Cell lysates were thawed and clarified at 15,000 $\times$ *g* for 15 min at 4°C. Aliquots of 250 μl of lysate were layered onto a 10 to 40% linear sucrose gradient. The sucrose gradients were spun in a Beckman ultracentrifuge at 150,000 $\times$ *g* for 2.5 h at 4°C. The gradients were fractionated and analyzed using a gradient fractionator (BioComp Instruments, Inc., NB, Canada).

Proteomics and RNA sequencing. Cultures of 60 ml of each strain were grown to log phase (OD_{600} ~0.4) and split into two parts to extract protein and RNA separately. Both aliquots were spun at 5,000 $\times$ *g* for 10 min. For proteomics, cells were resuspended in 500 μl of urea lysis buffer (8 M urea in 50 mM Tris [pH 8.2], 75 mM NaCl, Roche complete EDTA-free protease inhibitor cocktail tablet) and subjected to bead beating for 4 $\times$ 45 s with 3 min on ice in between. Cell lysates were spun down at 20,000 $\times$ *g* for 10 min at 4°C and the supernatant was isolated for proteomics sample preparation. For RNA sequencing, RNA was isolated as described previously (68), depleted for rRNA using RiboZero (Epicenter, Madison, WI), and prepared for sequencing using KAPA stranded RNA-Seq library preparation kit (Millipore Sigma, St. Louis, MO).

Quantitative proteomics. Samples for quantitative proteomics experiments were processed as described previously (69). Briefly, three biological replicates of each strain's lysates were reduced with 5 mM dithiothreitol (DTT), alkylated with 10 mM iodoacetamide (IAA), and digested with endoproteinase Lys-C (Wako Laboratories) for 2 h at a 1:50 enzyme to substrate ratio at 30°C, followed by an overnight digestion with trypsin (Promega, Madison, WI) at a 1:50 enzyme to substrate ratio at 37°C. Reactions were quenched with neat formic acid (FA) to a final concentration of 1%. Digests were desalted using tC18 SepPak reversed phase cartridges (Waters, Milford, MA) following the manufacturer's protocol. A tandem mass tag (TMT) isobaric labeling strategy was used for this experiment. An aliquot (50 μg) of each of the 9 samples were labeled by TMT10plex reagent (Thermo Fisher Scientific, Waltham, MA) following the manufacturer's protocol. A pooled reference standard was generated by mixing equal amounts of each of the nine samples and included in the tenth channel of the TMT10plex. Labeling efficiency was assessed prior to quenching the reactions. Once sufficient (>99%) labeling efficiency was achieved, reactions were quenched and samples were mixed together. Combined sample was desalted using tC18 Sep-Pac reversed-phase cartridges, and the eluate was dried down completely. Sample was reconstituted and fractionated on a Zorbax 300 Extend-C_{18} 4.6- by 250-mm column (Agilent Technologies, Santa Clara, CA), as described previously (69). Fractions were collected every minute during the gradient and further concatenated into a total of 24 fractions that were analyzed on a Q Exactive Plus mass spectrometer (MS) coupled to an EASY-nLC 1200 ultra-high-performance liquid chromatography (UHPLC) system (Thermo Fisher Scientific, Waltham, MA). One microgram of each of the fractions was injected on a 75-μm ID Picofrit column (New Objective, Woburn, MA) packed with Reprosil-Pur C_{18}-AQ 1.9 μm beads (Maisch, GmbH) in-house to a length of 22 cm. Sample was eluted at a 200-nl/min flow rate with solvent A of 0.1% FA–3% acetonitrile (ACN), solvent B of 0.1% FA–90% ACN and a gradient of 2 to 6% B in 1 min, 6 to 30% B in 84 min, 30 to 60% B in 9 min, 60 to 90% B in 1 min, and a hold at 90% B for 5 min. MS data were acquired in data-dependent mode with MS1 resolution of 70,000 and automatic gain control (AGC) of 3e6. MS/MS was performed on the most intense 12 ions with a resolution of 35,000, AGC of 5e4, isolation width of 1.6 amu, and normalized collision energy of 29. Data were extracted and searched against an *M. smegmatis* database using Spectrum Mill MS proteomics workbench (Agilent Technologies, Santa Clara, CA). Extracted spectra were searched using carbamidomethylation of cysteines and TMT labeling of N termini and lysine residues as fixed modifications and methionine oxidation, asparagine deamidation, and protein N-terminal acetylation as variable modifications. Spectrum to database matching was controlled with peptide level false discovery rate (FDR) of less than 1%. Peptides were rolled into protein groups and subgroups in Spectrum Mill with a protein level FDR of 0%. Protein summary export consisting of a list of quantified proteins with a reporter ion ratio of every TMT channel to the pooled reference channel was generated for quantitation of proteins. TMT10 reporter ion intensities were corrected for isotopic impurities in the Spectrum Mill protein/peptide summary module using the afRICA correction method, which implements determinant calculations according to Cramer's rule and correction factors obtained from the reagent manufacturer's certificate of analysis (https://www.thermofisher.com/order/catalog/product/90406) for lot number SE240163 (70). Proteins identified with 2 or more peptides were used for further statistical analysis. Comparisons of protein levels in each strain were assessed for significance using a two-sample moderated *t* test with an adjusted *P* value threshold of less than 0.05 for assessing significantly altered proteins. For visualization purposes in Fig. 2, the protein and RNA ratios associated with LepA were excluded from the volcano plot.

RNA sequencing. Samples were sequenced on an Illumina HiSeq 2500 in paired-end mode with a read length of 125 bp. Approximately 4 million reads were collected for each sample. Reads were mapped to the genome sequence of *M. smegmatis* mc^2 155 as a reference genome using Burrows-Wheeler aligner (BWA) (71). A Python script was used to separate reads in .sam files that mapped to the positive strand and negative strand of the chromosome. Then reads mapping to each open reading

frame (ORF) (in a strand-specific manner) were tabulated. The raw read counts were converted to fragments per kilobase per million reads (FPKMs) by dividing by gene length (in base pairs) and total reads in the sample and scaling up by 10^9. For analyses of differential gene expression, DESeq2 (72) was used to estimate log fold changes according to a hierarchical model based on the negative binomial distribution, and *P* values were calculated via a Wald test as a measure of significance. *P* values were adjusted for a false-discovery rate (FDR) of 5% over all genes by the Benjamini-Hochberg procedure.

Luciferase assays. Strains were grown to log phase and luciferase assays were conducted using Nanoglo luciferase assay system (Promega, Madison, WI). Briefly, 100 μl of cells was mixed with 100 μl of Nanoglo reagent (prepared as the kit protocol described). Within 2 min, luminescence measurements were taken in a TECAN Spark 10M plate reader with an integration time of 1,000 ms. The OD_{600} was also measured in each well, and luminescent values were normalized by OD_{600} to obtain relative luminescence values.

Porin knockdown and contribution to LepA phenotype. Strains were grown to log phase, diluted back into medium with or without aTc, and allowed to grow for 15 h to reach log phase. Cells were stained with calcein AM and analyzed by flow cytometry in biological triplicate, as described above.

Ethidium bromide uptake assay. Strains were grown to log phase, washed with phosphate-buffered saline (PBS)-0.4% glycerol (PBS-G) and prepared at an OD_{600} of 0.8. An aliquot of 100 μl of each strain was mixed with 100 μl of 4 μg/ml of ethidium bromide (prepared in PBS-G) in a 96-well plate. Fluorescence was measured in a TECAN Spark 10M plate reader, using an excitation of 520 nm and emission of 600 nm.

Fluorescence microscopy and image analysis. GroEL-Dendra2 and MmpL3-Dendra2 strains were a gift from the Mycobacterial Systems Resource (principal investigator, K. Derbshire). Live still imaging of MspA-mRFP and Dendra2 fusion strains was performed using a Nikon TI-E inverted, wide-field microscope equipped with a Plan Apo 100×, 1.45-numerical-aperture (NA) objective, Spectra X LED light source, and an Andor Zyla sCMOS camera. *M. smegmatis* samples were spotted on 2% agarose pads. NIS-Elements version 4.5 software was used for data acquisition and ImageJ software was used for processing.

Experimental replicates. Unless otherwise noted all experiments were conducted at least twice, in biological triplicate.

Data analysis. Protein functional enrichment analysis was performed using "Functional Annotation" software within the DAVID platform (https://david.ncifcrf.gov/home.jsp). Specifically, InterPro terms considered biologically significant, and therefore visualized, refer to at least 6 proteins in the list of 80 proteins significantly altered by LepA. Statistical significance was determined using a modified Fisher's exact test (35). All other statistical measurements and tests are specified in the figure legends.

mRNA quantification. mRNA was quantified as described previously (44). Briefly, purified RNA (DNase treated) was used as the template for cDNA synthesis, following the manufacturer's instructions with Superscript V (Life Technologies, Carlsbad, CA). RNA was removed from the reaction using alkaline hydrolysis and the cDNA was cleaned using column purification (Zymo Research, Irvine, CA). Quantitative PCR (qPCR) was performed on purified cDNA using iTaq Universal SYBR green Supermix (Bio-Rad, Hercules, CA). mRNA fold change was calculated using the threshold cycle ($\Delta\Delta C_T$) method, where porin transcript level was normalized by *sigA* level in each genetic background.

Data availability. The original mass spectra and sequence database have been deposited in the public proteomics repository MassIVE and are accessible at ftp://MSV000083513@massive.ucsd.edu when providing the data set password "mycobacteria."

The RNA-seq raw sequence files are deposited at BioProject accession number PRJNA518044, and the gene expression levels (FPKMs) are deposited in GEO under accession number GSE126130.

The further data that support these findings are available from the corresponding author upon reasonable request.

SUPPLEMENTAL MATERIAL

Supplemental material is available online only.

SUPPLEMENTAL FILE 1, XLSX file, 1.1 MB.

SUPPLEMENTAL FILE 2, XLSX file, 6.4 MB.

SUPPLEMENTAL FILE 3, PDF file, 2.2 MB.

ACKNOWLEDGMENTS

We thank Allison Carey and Thibault Barbier for advice on the manuscript. We also thank Allen Buskirk for his reading of the manuscript. We thank Sarah Fortune and the Fortune lab for insightful discussion on the work. We thank Bill Neidermeyer and members of the Whelan lab for allowing us to use ribosome fractionation machinery. We are grateful to the Michael Welsh and the Walker lab for allowing us to use their protein purification equipment.

This research was supported by funding from the NIH/NIAID (U19 AI107774 and P01 AI095208 to E.J.R.). The DNA Resource Core of Dana-Farber/Harvard Cancer Center, where sequencing reactions were carried out, was funded in part by NCI Cancer Center support grant 2P30CA006516-48.

Author contributions are as follows. Conceptualization: S.R.S.F, F.G.T., E.H.R, C.L.D, and E.J.R.; Methodology: S.R.S.F, F.G.T, E.H.R, C.L.D, E.J.R, H.K., T.R.I, and S.A.C.; Investigation: S.R.S.F, F.G.T, E.H.R, I.D.W, A.W, L.W., H.K., and T.R.I.; Data Curation: S.R.S.F, H.K., and T.R.I.; Writing—Original Draft: S.R.S.F, F.G.T, E.H.R, and E.J.R.; Writing—Review & Editing: S.R.S.F, F.G.T, E.H.R, E.J.R., H.K., T.R.I., S.A.C., C.L.D, and I.D.W.

We have no conflicts of interest to declare.

REFERENCES

1. Kerantzas CA, Jacobs WR, Jr. 2017. Origins of combination therapy for tuberculosis: lessons for future antimicrobial development and application. mBio 8:e01586-16. https://doi.org/10.1128/mBio.01586-16.
2. Harding E. 2020. WHO global progress report on tuberculosis elimination. Lancet Respir Med 8:19. https://doi.org/10.1016/S2213-2600(19)30418-7.
3. Sarathy J, Dartois V, Dick T, Gengenbacher M. 2013. Reduced drug uptake in phenotypically resistant nutrient-starved nonreplicating Mycobacterium tuberculosis. Antimicrob Agents Chemother 57:1648–1653. https://doi.org/10.1128/AAC.02202-12.
4. Jackson M, Raynaud C, Laneelle MA, Guilhot C, Laurent-Winter C, Ensergueix D, Gicquel B, Daffe M. 1999. Inactivation of the antigen 85C gene profoundly affects the mycolate content and alters the permeability of the Mycobacterium tuberculosis cell envelope. Mol Microbiol 31:1573–1587. https://doi.org/10.1046/j.1365-2958.1999.01310.x.
5. Dulberger CL, Rubin EJ, Boutte CC. 2020. The mycobacterial cell envelope—a moving target. Nat Rev Microbiol 18:47–59. https://doi.org/10.1038/s41579-019-0273-7.
6. Kieser KJ, Rubin EJ. 2014. How sisters grow apart: mycobacterial growth and division. Nat Rev Microbiol 12:550–562. https://doi.org/10.1038/nrmicro3299.
7. Vogel C, Marcotte EM. 2012. Insights into the regulation of protein abundance from proteomic and transcriptomic analyses. Nat Rev Genet 13:227–232. https://doi.org/10.1038/nrg3185.
8. Brar GA, Weissman JS. 2015. Ribosome profiling reveals the what, when, where and how of protein synthesis. Nat Rev Mol Cell Biol 16:651–664. https://doi.org/10.1038/nrm4069.
9. Pechmann S, Chartron JW, Frydman J. 2014. Local slowdown of translation by nonoptimal codons promotes nascent-chain recognition by SRP in vivo. Nat Struct Mol Biol 21:1100–1105. https://doi.org/10.1038/nsmb.2919.
10. Flygaard RK, Boegholm N, Yusupov M, Jenner LB. 2018. Cryo-EM structure of the hibernating Thermus thermophilus 100S ribosome reveals a protein-mediated dimerization mechanism. Nat Commun 9:4179. https://doi.org/10.1038/s41467-018-06724-x.
11. Chen YX, Xu ZY, Ge X, Sanyal S, Lu ZJ, Javid B. 2020. Selective translation by alternative bacterial ribosomes. Proc Natl Acad Sci U S A 117:19487–-19496. https://doi.org/10.1073/pnas.2009607117.
12. Herskovits AA, Bibi E. 2000. Association of Escherichia coli ribosomes with the inner membrane requires the signal recognition particle receptor but is independent of the signal recognition particle. Proc Natl Acad Sci U S A 97:4621–4626. https://doi.org/10.1073/pnas.080077197.
13. Schibich D, Gloge F, Pohner I, Bjorkholm P, Wade RC, von Heijne G, Bukau B, Kramer G. 2016. Global profiling of SRP interaction with nascent polypeptides. Nature 536:219–223. https://doi.org/10.1038/nature19070.
14. Oh E, Becker AH, Sandikci A, Huber D, Chaba R, Gloge F, Nichols RJ, Typas A, Gross CA, Kramer G, Weissman JS, Bukau B. 2011. Selective ribosome profiling reveals the cotranslational chaperone action of trigger factor in vivo. Cell 147:1295–1308. https://doi.org/10.1016/j.cell.2011.10.044.
15. Sawyer EB, Grabowska AD, Cortes T. 2018. Translational regulation in mycobacteria and its implications for pathogenicity. Nucleic Acids Res 46:6950–6961. https://doi.org/10.1093/nar/gky574.
16. Rudra P, Hurst-Hess KR, Cotten KL, Partida-Miranda A, Ghosh P. 2020. Mycobacterial HflX is a ribosome splitting factor that mediates antibiotic resistance. Proc Natl Acad Sci U S A 117:629–634. https://doi.org/10.1073/pnas.1906748117.
17. Li Y, Corro JH, Palmer CD, Ojha AK. 2020. Progression from remodeling to hibernation of ribosomes in zinc-starved mycobacteria. Proc Natl Acad Sci U S A 117:19528–19537. https://doi.org/10.1073/pnas.2013409117.
18. Rego EH, Audette RE, Rubin EJ. 2017. Deletion of a mycobacterial divisome factor collapses single-cell phenotypic heterogeneity. Nature 546:153–157. https://doi.org/10.1038/nature22361.
19. Qin Y, Polacek N, Vesper O, Staub E, Einfeldt E, Wilson DN, Nierhaus KH. 2006. The highly conserved LepA is a ribosomal elongation factor that back-translocates the ribosome. Cell 127:721–733. https://doi.org/10.1016/j.cell.2006.09.037.
20. Heller JLE, Kamalampeta R, Wieden HJ. 2017. Taking a step back from back-translocation: an integrative view of LepA/EF4's cellular function. Mol Cell Biol 37:e00653-16. https://doi.org/10.1128/MCB.00653-16.
21. Youngman EM, Green R. 2007. Ribosomal translocation: LepA does it backwards. Curr Biol 17:R136–9. https://doi.org/10.1016/j.cub.2006.12.029.
22. Ji DL, Lin H, Chi W, Zhang LX. 2012. CpLEPA is critical for chloroplast protein synthesis under suboptimal conditions in Arabidopsis thaliana. PLoS One 7:e49746. https://doi.org/10.1371/journal.pone.0049746.
23. Bauerschmitt H, Funes S, Herrmann JM. 2008. The membrane-bound GTPase Guf1 promotes mitochondrial protein synthesis under suboptimal conditions. J Biol Chem 283:17139–17146. https://doi.org/10.1074/jbc.M710037200.
24. Badu-Nkansah A, Sello JK. 2010. Deletion of the elongation factor 4 gene (lepA) in Streptomyces coelicolor enhances the production of the calcium-dependent antibiotic. FEMS Microbiol Lett 311:147–151. https://doi.org/10.1111/j.1574-6968.2010.02083.x.
25. Kida Y, Shimizu T, Kuwano K. 2011. Cooperation between LepA and PlcH contributes to the in vivo virulence and growth of Pseudomonas aeruginosa in mice. Infect Immun 79:211–219. https://doi.org/10.1128/IAI.01053-10.
26. Shoji S, Janssen BD, Hayes CS, Fredrick K. 2010. Translation factor LepA contributes to tellurite resistance in Escherichia coli but plays no apparent role in the fidelity of protein synthesis. Biochimie 92:157–163. https://doi.org/10.1016/j.biochi.2009.11.002.
27. Zhu P, Liu Y, Zhang F, Bai X, Chen Z, Shangguan F, Zhang B, Zhang L, Chen Q, Xie D, Lan L, Xue X, Liang XJ, Lu B, Wei T, Qin Y. 2018. Human elongation factor 4 regulates cancer bioenergetics by acting as a mitochondrial translation switch. Cancer Res 78:2813–2824. https://doi.org/10.1158/0008-5472.CAN-17-2059.
28. Balakrishnan R, Oman K, Shoji S, Bundschuh R, Fredrick K. 2014. The conserved GTPase LepA contributes mainly to translation initiation in Escherichia coli. Nucleic Acids Res 42:13370–13383. https://doi.org/10.1093/nar/gku1098.
29. Gibbs MR, Moon KM, Chen M, Balakrishnan R, Foster LJ, Fredrick K. 2017. Conserved GTPase LepA (Elongation Factor 4) functions in biogenesis of the 30S subunit of the 70S ribosome. Proc Natl Acad Sci U S A 114:980–985. https://doi.org/10.1073/pnas.1613665114.
30. Liu H, Chen C, Zhang H, Kaur J, Goldman YE, Cooperman BS. 2011. The conserved protein EF4 (LepA) modulates the elongation cycle of protein synthesis. Proc Natl Acad Sci U S A 108:16223–16228. https://doi.org/10.1073/pnas.1103820108.
31. Zhang D, Yan K, Liu G, Song G, Luo J, Shi Y, Cheng E, Wu S, Jiang T, Lou J, Gao N, Qin Y. 2016. EF4 disengages the peptidyl-tRNA CCA end and facilitates back-translocation on the 70S ribosome. Nat Struct Mol Biol 23:125–131. https://doi.org/10.1038/nsmb.3160.
32. Gagnon MG, Lin J, Steitz TA. 2016. Elongation factor 4 remodels the A-site tRNA on the ribosome. Proc Natl Acad Sci U S A 113:4994–4999. https://doi.org/10.1073/pnas.1522932113.
33. Evans RN, Blaha G, Bailey S, Steitz TA. 2008. The structure of LepA, the ribosomal back translocase. Proc Natl Acad Sci U S A 105:4673–4678. https://doi.org/10.1073/pnas.0801308105.
34. Wu KJ, Boutte CC, Ioerger TR, Rubin EJ. 2019. Mycobacterium smegmatis HtrA blocks the toxic activity of a putative cell wall amidase. Cell Rep 27:2468–2479. https://doi.org/10.1016/j.celrep.2018.12.063.
35. Huang da W, Sherman BT, Lempicki RA. 2009. Systematic and integrative analysis of large gene lists using DAVID bioinformatics resources. Nat Protoc 4:44–57. https://doi.org/10.1038/nprot.2008.211.
36. Stahl C, Kubetzko S, Kaps I, Seeber S, Engelhardt H, Niederweis M. 2001. MspA provides the main hydrophilic pathway through the cell wall of

Mycobacterium smegmatis. Mol Microbiol 40:451–464. https://doi.org/10.1046/j.1365-2958.2001.02394.x.
37. Hermann C, Giddey AD, Nel AJM, Soares NC, Blackburn JM. 2019. Cell wall enrichment unveils proteomic changes in the cell wall during treatment of Mycobacterium smegmatis with sub-lethal concentrations of rifampicin. J Proteomics 191:166–179. https://doi.org/10.1016/j.jprot.2018.02.019.
38. Heinz C, Niederweis M. 2000. Selective extraction and purification of a mycobacterial outer membrane protein. Anal Biochem 285:113–120. https://doi.org/10.1006/abio.2000.4728.
39. Mahfoud M, Sukumaran S, Hulsmann P, Grieger K, Niederweis M. 2006. Topology of the porin MspA in the outer membrane of Mycobacterium smegmatis. J Biol Chem 281:5908–5915. https://doi.org/10.1074/jbc.M511642200.
40. Niederweis M, Ehrt S, Heinz C, Klocker U, Karosi S, Swiderek KM, Riley LW, Benz R. 1999. Cloning of the mspA gene encoding a porin from Mycobacterium smegmatis. Mol Microbiol 33:933–945. https://doi.org/10.1046/j.1365-2958.1999.01472.x.
41. Stephan J, Bender J, Wolschendorf F, Hoffmann C, Roth E, Mailander C, Engelhardt H, Niederweis M. 2005. The growth rate of Mycobacterium smegmatis depends on sufficient porin-mediated influx of nutrients. Mol Microbiol 58:714–730. https://doi.org/10.1111/j.1365-2958.2005.04878.x.
42. Danilchanka O, Pavlenok M, Niederweis M. 2008. Role of porins for uptake of antibiotics by Mycobacterium smegmatis. Antimicrob Agents Chemother 52:3127–3134. https://doi.org/10.1128/AAC.00239-08.
43. Svetlikova Z, Skovierova H, Niederweis M, Gaillard JL, McDonnell G, Jackson M. 2009. Role of porins in the susceptibility of Mycobacterium smegmatis and Mycobacterium chelonae to aldehyde-based disinfectants and drugs. Antimicrob Agents Chemother 53:4015–4018. https://doi.org/10.1128/AAC.00590-09.
44. Rock JM, Hopkins FF, Chavez A, Diallo M, Chase MR, Gerrick ER, Pritchard JR, Church GM, Rubin EJ, Sassetti CM, Schnappinger D, Fortune SM. 2017. Programmable transcriptional repression in mycobacteria using an orthogonal CRISPR interference platform. Nat Microbiol 2:16274. https://doi.org/10.1038/nmicrobiol.2016.274.
45. Rodrigues L, Ramos J, Couto I, Amaral L, Viveiros M. 2011. Ethidium bromide transport across Mycobacterium smegmatis cell-wall: correlation with antibiotic resistance. BMC Microbiol 11:35. https://doi.org/10.1186/1471-2180-11-35.
46. Stephan J, Mailaender C, Etienne G, Daffe M, Niederweis M. 2004. Multidrug resistance of a porin deletion mutant of Mycobacterium smegmatis. Antimicrob Agents Chemother 48:4163–4170. https://doi.org/10.1128/AAC.48.11.4163-4170.2004.
47. Jones CM, Niederweis M. 2010. Role of porins in iron uptake by Mycobacterium smegmatis. J Bacteriol 192:6411–6417. https://doi.org/10.1128/JB.00986-10.
48. Niederweis M. 2008. Nutrient acquisition by mycobacteria. Microbiology (Reading) 154:679–692. https://doi.org/10.1099/mic.0.2007/012872-0.
49. Wolschendorf F, Mahfoud M, Niederweis M. 2007. Porins are required for uptake of phosphates by Mycobacterium smegmatis. J Bacteriol 189:2435–2442. https://doi.org/10.1128/JB.01600-06.
50. Kieser KJ, Baranowski C, Chao MC, Long JE, Sassetti CM, Waldor MK, Sacchettini JC, Ioerger TR, Rubin EJ. 2015. Peptidoglycan synthesis in Mycobacterium tuberculosis is organized into networks with varying drug susceptibility. Proc Natl Acad Sci U S A 112:13087–13092. https://doi.org/10.1073/pnas.1514135112.
51. Zhang YJ, Reddy MC, Ioerger TR, Rothchild AC, Dartois V, Schuster BM, Trauner A, Wallis D, Galaviz S, Huttenhower C, Sacchettini JC, Behar SM, Rubin EJ. 2013. Tryptophan biosynthesis protects mycobacteria from CD4 T-cell-mediated killing. Cell 155:1296–1308. https://doi.org/10.1016/j.cell.2013.10.045.
52. Siegrist MS, Unnikrishnan M, McConnell MJ, Borowsky M, Cheng TY, Siddiqi N, Fortune SM, Moody DB, Rubin EJ. 2009. Mycobacterial Esx-3 is required for mycobactin-mediated iron acquisition. Proc Natl Acad Sci U S A 106:18792–18797. https://doi.org/10.1073/pnas.0900589106.
53. Bottai D, Di Luca M, Majlessi L, Frigui W, Simeone R, Sayes F, Bitter W, Brennan MJ, Leclerc C, Batoni G, Campa M, Brosch R, Esin S. 2012. Disruption of the ESX-5 system of Mycobacterium tuberculosis causes loss of PPE protein secretion, reduction of cell wall integrity and strong attenuation. Mol Microbiol 83:1195–1209. https://doi.org/10.1111/j.1365-2958.2012.08001.x.
54. Li GW, Burkhardt D, Gross C, Weissman JS. 2014. Quantifying absolute protein synthesis rates reveals principles underlying allocation of cellular resources. Cell 157:624–635. https://doi.org/10.1016/j.cell.2014.02.033.
55. De Laurentiis EI, Wieden HJ. 2015. Identification of two structural elements important for ribosome-dependent GTPase activity of elongation factor 4 (EF4/LepA). Sci Rep 5:8573. https://doi.org/10.1038/srep08573.
56. Hillmann D, Eschenbacher I, Thiel A, Niederweis M. 2007. Expression of the major porin gene mspA is regulated in Mycobacterium smegmatis. J Bacteriol 189:958–967. https://doi.org/10.1128/JB.01474-06.
57. Riba A, Di Nanni N, Mittal N, Arhne E, Schmidt A, Zavolan M. 2019. Protein synthesis rates and ribosome occupancies reveal determinants of translation elongation rates. Proc Natl Acad Sci U S A 116:15023–15032. https://doi.org/10.1073/pnas.1817299116.
58. Shieh YW, Minguez P, Bork P, Auburger JJ, Guilbride DL, Kramer G, Bukau B. 2015. Operon structure and cotranslational subunit association direct protein assembly in bacteria. Science 350:678–680. https://doi.org/10.1126/science.aac8171.
59. Butkus ME, Prundeanu LB, Oliver DB. 2003. Translocon "pulling" of nascent SecM controls the duration of its translational pause and secretion-responsive secA regulation. J Bacteriol 185:6719–6722. https://doi.org/10.1128/jb.185.22.6719-6722.2003.
60. Fluman N, Navon S, Bibi E, Pilpel Y. 2014. mRNA-programmed translation pauses in the targeting of E. coli membrane proteins. Elife 3:e03440. https://doi.org/10.7554/eLife.03440.
61. Mercier E, Holtkamp W, Rodnina MV, Wintermeyer W. 2017. Signal recognition particle binds to translating ribosomes before emergence of a signal anchor sequence. Nucleic Acids Res 45:11858–11866. https://doi.org/10.1093/nar/gkx888.
62. Gao Y, Bai X, Zhang D, Han C, Yuan J, Liu W, Cao X, Chen Z, Shangguan F, Zhu Z, Gao F, Qin Y. 2016. Mammalian elongation factor 4 regulates mitochondrial translation essential for spermatogenesis. Nat Struct Mol Biol 23:441–449. https://doi.org/10.1038/nsmb.3206.
63. Gibson DG, Young L, Chuang R-Y, Venter JC, Hutchison CA, Smith HO. 2009. Enzymatic assembly of DNA molecules up to several hundred kilobases. Nat Methods 6:343–345. https://doi.org/10.1038/nmeth.1318.
64. Murphy KC, Papavinasasundaram K, Sassetti CM. 2015. Mycobacterial recombineering. Methods Mol Biol 1285:177–199. https://doi.org/10.1007/978-1-4939-2450-9_10.
65. van Kessel JC, Hatfull GF. 2008. Mycobacterial recombineering. Methods Mol Biol 435:203–215. https://doi.org/10.1007/978-1-59745-232-8_15.
66. Baranowski C, Welsh MA, Sham LT, Eskandarian HA, Lim HC, Kieser KJ, Wagner JC, McKinney JD, Fantner GE, Ioerger TR, Walker S, Bernhardt TG, Rubin EJ, Rego EH. 2018. Maturing Mycobacterium smegmatis peptidoglycan requires non-canonical crosslinks to maintain shape. Elife 7:e37516. https://doi.org/10.7554/eLife.37516.
67. Mohammad F, Green R, Buskirk AR. 2019. A systematically-revised ribosome profiling method for bacteria reveals pauses at single-codon resolution. Elife 8:e42591. https://doi.org/10.7554/eLife.42591.
68. Gerrick ER, Barbier T, Chase MR, Xu R, Francois J, Lin VH, Szucs MJ, Rock JM, Ahmad R, Tjaden B, Livny J, Fortune SM. 2018. Small RNA profiling in Mycobacterium tuberculosis identifies MrsI as necessary for an anticipatory iron sparing response. Proc Natl Acad Sci U S A 115:6464–6469. https://doi.org/10.1073/pnas.1718003115.
69. Mertins P, Tang LC, Krug K, Clark DJ, Gritsenko MA, Chen L, Clauser KR, Clauss TR, Shah P, Gillette MA, Petyuk VA, Thomas SN, Mani DR, Mundt F, Moore RJ, Hu Y, Zhao R, Schnaubelt M, Keshishian H, Monroe ME, Zhang Z, Udeshi ND, Mani D, Davies SR, Townsend RR, Chan DW, Smith RD, Zhang H, Liu T, Carr SA. 2018. Reproducible workflow for multiplexed deep-scale proteome and phosphoproteome analysis of tumor tissues by liquid chromatography-mass spectrometry. Nat Protoc 13:1632–1661. https://doi.org/10.1038/s41596-018-0006-9.
70. Shadforth I, Dunkley T, Lilley K, Crowther D, Bessant C. 2005. Confident protein identification using the average peptide score method coupled with search-specific, ab initio thresholds. Rapid Commun Mass Spectrom 19:3363–3368. https://doi.org/10.1002/rcm.2203.
71. Li H, Durbin R. 2009. Fast and accurate short read alignment with Burrows-Wheeler transform. Bioinformatics 25:1754–1760. https://doi.org/10.1093/bioinformatics/btp324.
72. Love MI, Huber W, Anders S. 2014. Moderated estimation of fold change and dispersion for RNA-seq data with DESeq2. Genome Biol 15:550. https://doi.org/10.1186/s13059-014-0550-8.